Magnetic Resonance Field Fingerprinting (MRF²)

Gregor Körzdörfer[1,2]; Yun Jiang[3]; Jianing Pang[4]; Peter Speier[1]; Vikas Gulani[3,5]; Mark Griswold[3,5]; Mathias Nittka[1]

[1] Siemens Healthineers, Erlangen, Germany
[2] Friedrich-Alexander-Universität Erlangen-Nürnberg, Erlangen, Germany
[3] Radiology, Case Western Reserve University, Cleveland, OH, USA
[4] Siemens Medical Solutions USA, Inc., Chicago, IL, USA
[5] Biomedical Engineering, Case Western Reserve University, Cleveland, OH, USA

Magnetic Resonance Fingerprinting

Magnetic resonance fingerprinting (MRF)[1] [1] is a recently introduced technique that promises multiparametric quantitative MRI. In essence, MRF aims to identify multiple tissue properties simultaneously in a single acquisition. To do so, a measured signal is compared to a set (or "dictionary") of pre-simulated signals. Each signal is unique, and can therefore be considered a kind of fingerprint. By comparing a measured fingerprint with the dictionary entries, the most similar simulated fingerprint is identified. This reveals the measured fingerprint's properties, which are the parameters that were used for the simulation.

The interaction of two main characteristics of MRF plays an important role. First, MRF encoding patterns aim to generate highly variable signal responses from tissues with different properties. This is different from conventional imaging, which aims for highly specific tissue contrasts. Second, a pattern-matching process is used to identify the parameters of the measured signals. This makes MRF independent of analytical models and means that signals

[1] WIP. The product is still under development and is not commercially available yet. Its future availability cannot be ensured.

1

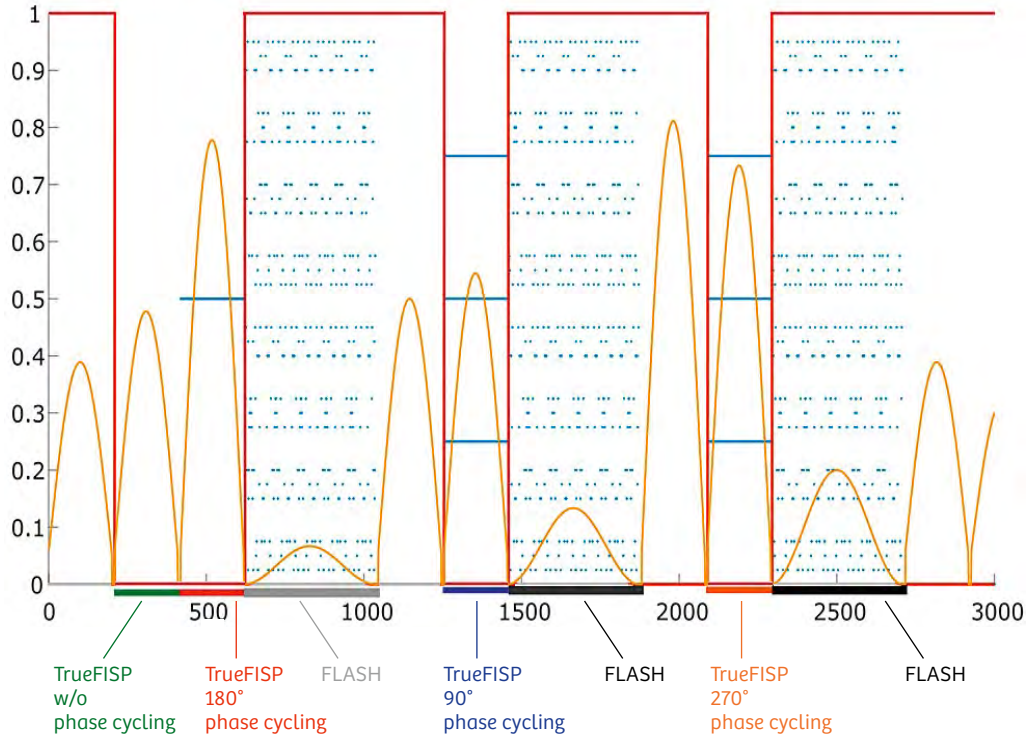

Figure 1:
Sequence configuration used for MRF² showing flip angle, z-gradient moment at the end of the TR, and the pulse phase. The TrueFISP segments are also described by their phase cycling pattern.

are designed by exploiting many more degrees of freedom. Highly distinguishable, complex signal responses can be generated with a series of RF pulses – in contrast to conventional sequences, which require a steady-state signal. The combination of high distinguishability and the pattern-matching approach opens up the possibility of strong undersampling during data acquisition. While all *k*-space data would have to be acquired to generate artifact-free images of each time point, MRF only acquires a small fraction of the data. The *k*-space sampling patterns can be so sparse that a single image barely shows the underlying object. By varying the *k*-space sampling pattern in a reasonable manner from time point to time point, the resulting artifacts that overlie the signal also vary and do not affect the pattern match. Even though the measured signals are heavily affected by artifacts, the algorithm can still find the best fingerprint match in each voxel. This is mostly performed by a voxel-wise pattern match, but can also be achieved with more sophisticated techniques [e.g., 2–4].

In general, any sequence in combination with any *k*-space sampling scheme (Cartesian, radial, spiral, etc.) could be applied for MRF. When choosing a suitable sequence, one has to keep in mind that specific sequence properties are also present in MRF. Ma et al. showed a first working imple-mentation based on a TrueFISP sequence with spiral sampling yielding B_0, T1, and T2 parameter maps [1]. TrueFISP has high signal efficiency but suffers from problems linked to B_0 inhomogeneities, which result in banding artifacts. Although the signal can be simulated accurately under such conditions, a low signal-to-noise ratio can severely affect the MRF results with systematic biases or higher standard deviation in the parameter maps. The original method was therefore followed by the FISP-based approach devised by Jiang et al. [5]. This method does not incorporate B_0 in the signal model, as FISP has negligible B_0 dependency. Several works [6, 7] identified a dependency of the parameter maps on the RF transmit field B_1+ that probably also exists in the TrueFISP MRF method. This can be addressed with a B_1+ prescan [7–9] as a brute-force approach. A more elegant solution would be to also incorporate B_1+ in the encoding and matching, which can be done by integrating dedicated B_1+ dependent signal segments in an encoding pattern [6, 10]. Instead of fighting artifacts that are related to magnetic field inhomoge-neities, MRF can embrace them. B_0 and B_1+ can also be simultaneously identified in addition to parameters associated with the underlying tissues, such as T1 and T2. This is necessary in cases where the signal behavior is influenced by variations in one or both of the magnetic fields. Mismatches can appear when the signal is affected in a way that makes it more closely resemble a signal with different tissue para-meters. By simultaneously mapping spatial magnetic field distributions, such mismatches can be resolved, and MRF can generate parameter maps that are free of influences from the underlying magnetic fields.

Magnetic Resonance Field Fingerprinting (MRF²)

Magnetic resonance field fingerprinting (MRF²)[1] follows the MRF idea and attempts to generate B_0, B_1+, T1, and T2 maps from a single continuous acquisition. As MRF does not rely on a steady-state, there is theoretically no need to use a single sequence framework throughout an acquisition. MRF² uses different sequence types and thus benefits from exploiting more degrees of freedom. By varying flip angles, pulse phases, and gradient moments, a sequence is designed that integrates FLASH, FISP, and TrueFISP segments into one continuous acquisition (Fig. 1). Each sequence differs in its sensitivity to tissue parameters and magnetic fields. FISP is mainly sensitive to T1, T2, and B_1+, while FLASH is sensitive to T1 and B_1+, and TrueFISP is sensitive to T1, T2, B_0, and B_1. In MRF², the TrueFISP related limitations are being dealt with by also using sequences that are less B_0-dependent and complementing it by varying the phase cycling pattern in the TrueFISP segments. Low signal levels in one TrueFISP segment are offset by other TrueFISP segments, and by FISP and FLASH segments. Figure 2 shows examples of MRF² parameter maps in a healthy volunteers' brain.

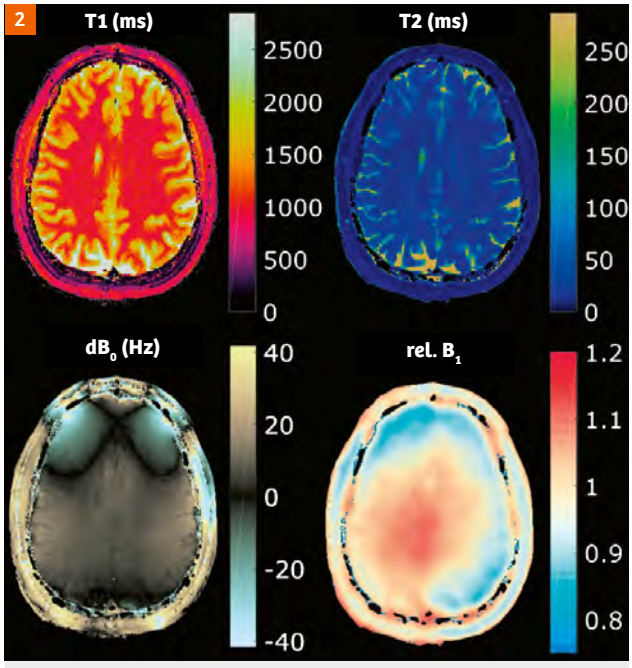

Figure 2:
T1, T2, B_0 and B_1+ maps obtained using MRF² in a healthy volunteer brain (FOV: 230 mm; undersampling factor: 48; in-plane resolution: 0.9 mm: slice thickness: 5 mm).

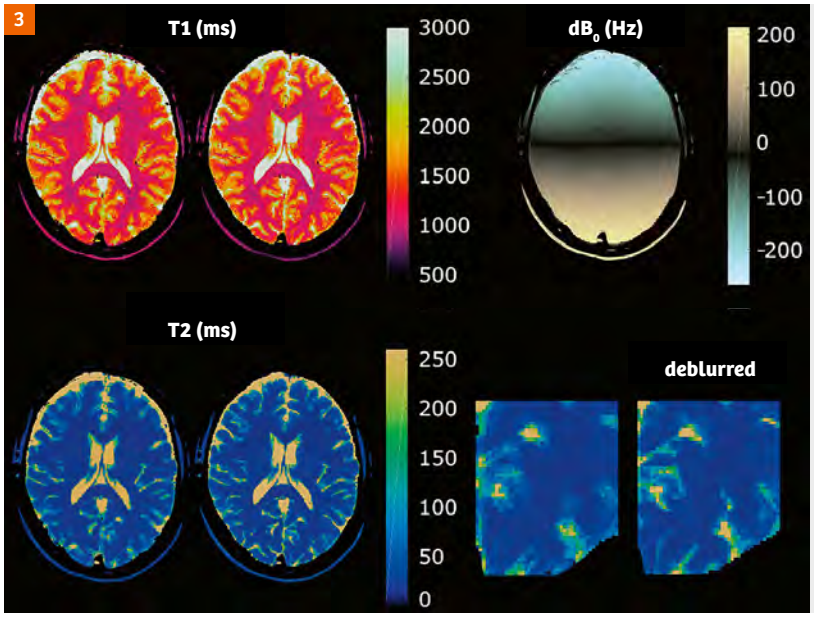

Figure 3:
A human brain acquired using MRF² with an additional B_0 shim in y-direction, as shown in the top right (FOV: 230 mm; undersampling factor: 48; in-plane resolution: 0.9 mm; slice thickness: 5 mm). The image in the bottom right compares the resulting MRF² T1 and T2 maps with and without deblurring using the B_0 map with zoomed-in T2 maps.

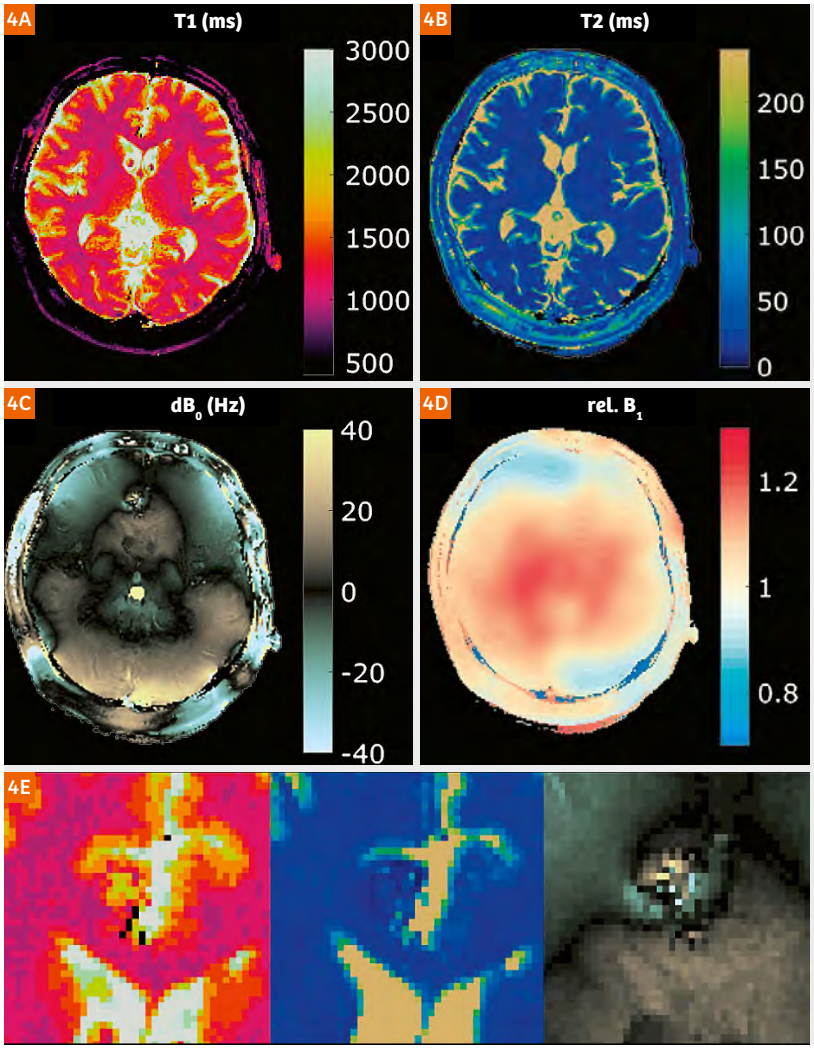

Figure 4:
MRF² parameter maps (undersampling factor: 48; in-plane resolution: 1.2 mm; slice thickness: 5 mm) in a volunteer with a diagnosed cavernoma. The images show T1/T2 changes in the cavernoma compared to the surrounding white matter, and abrupt changes in B_0. A zoomed excerpt of the cavernoma is shown in 4E.

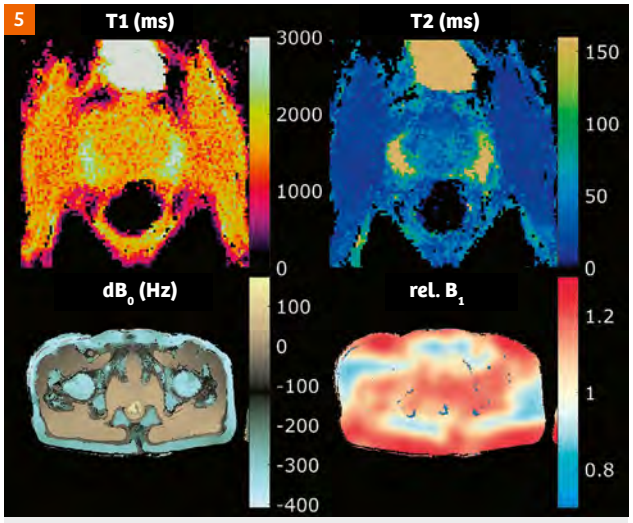

Figure 5:
Parameter maps (undersampling factor: 60; in-plane resolution: 1 mm; slice thickness: 3.5 mm) in a volunteer's prostate. Zoomed-in versions of the T1 and T2 maps are shown, as well as B_0 and B_1+ in the whole abdomen.

Another important factor in MRF is the dictionary size. Adding dimension exponentially increases the number of fingerprints. Since the simulation tries to accurately resemble MR physics on a macroscopic level, this is a time-consuming task. Although investing this time is bearable because the dictionary must only be computed once for a given sequence, having more fingerprints means that it takes more memory and time to match each acquired dataset. The four orthogonal dimensions in MRF² result in a very large dictionary. To minimize the size, the TR is kept constant to limit the extent of the B_0 dimension: Keeping the TR constant means that two spin ensembles with a frequency difference of an integer multiple of 1/TR will experience almost the same evolution. Therefore, the dictionary size can be substan-tially limited to the range of +-2/TR Hz. The downside of limiting the B_0 dimension is that wraparounds appear in the B_0 dimension. Although the parameter maps are free of influences from B_0, the full scale B_0 cannot be identified. In order to assess higher off-resonances, the echo time in two of the FISP segments is slightly different but constant throughout one segment. The resulting phase differences serve to compute a coarse B_0 map for unwrapping.

High overall signal levels and good distinguishability of fingerprints with MRF² enable high resolutions. Derived B_0 maps can be used for spiral deburring (Fig. 3) and, as a measure of susceptibility, for diagnostic information. Figure 4 shows a volunteer's brain with a diagnosed cavernoma. Besides higher T1 and lower T2 signals inside the cavernoma compared to the surrounding white matter, abrupt changes in the B_0 are visible. Figure 5 displays MRF² results from another body region. B_0 and B_1+ maps in the abdomen are shown as well as zoomed-in T1 and T2 maps in the prostate only. Pixels containing fat were removed based on the off-resonance map.

Summary

MRF² extends the concept of MRF by simultaneously identifying both magnetic fields and relaxation parameter maps. It is therefore highly robust against field variations, and yields additional information to relaxation parameter maps. Signal changes related to B_0 and B_1+ are intrinsically accounted for by adding a B_1+ and B_0 dimension to the dictionary with subsequent matching of these field parameters. Higher signal levels, better distinguishability between fingerprints, and integrated spiral deblurring help achieve higher resolutions. The high-resolution B_0 information that is related to susceptibility can also be used for diagnosis.

References

1 Ma D, Gulani V, Seiberlich N, et al. Magnetic resonance fingerprinting. Nature 2013;495(7440):187-192. doi: 10.1038/nature11971.
2 Cline CC, Chen X, Mailhe B, et al. AIR-MRF: Accelerated iterative reconstruction for magnetic resonance fingerprinting. Magn Reson Imaging 2017;41:29-40. doi: 10.1016/j.mri.2017.07.007.
3 Zhao B, Lu W, Hitchens TK, et al. Accelerated MR parameter mapping with low-rank and sparsity constraints. Magn Reson Med. 2015;74(2):489-98. doi: 10.1002/mrm.25421.
4 Assländer J, Cloos MA, Knoll F, et al. Low rank alternating direction method of multipliers reconstruction for MR fingerprinting. Magn Reson Med. 2017;79(1):83-96. doi: 10.1002/mrm.26639.
5 Jiang Y, Ma D, Seiberlich N, et al. MR fingerprinting using fast imaging with steady state precession (FISP) with spiral readout. Magn Reson Med. 2015;74(6):1621-31. doi: 10.1002/mrm.26048.
6 Buonincontri G, Sawiak SJ. MR fingerprinting with simultaneous B1 estimation. Magn Reson Med. 2016;76(4):1127-1135. doi: 10.1002/mrm.26009.
7 Chen Y, Jiang Y, Pahwa S, et al. MR Fingerprinting for Rapid Quantitative Abdominal Imaging. Radiology 2016;279(1):278-286. doi: 10.1148/radiol.2016152037.
8 Ma D, Jiang Y, Chen Y, et al. Fast 3D magnetic resonance fingerprinting for a whole-brain coverage. Magn Reson Med. 2017;79(4):2190–2197. doi: 10.1002/mrm.26886.
9 Ma D, Coppo S, Chen Y, et al. Slice profile and B1 corrections in 2D magnetic resonance fingerprinting. Magn Reson Med. 2017;78(5):1781-1789. doi: 10.1002/mrm.26580.
10 Cloos MA, Knoll F, Zhao T, et al. Multiparametric imaging with heterogeneous radiofrequency fields. Nat Commun. 2016;7:12445. doi: 10.1038/ncomms12445.

Contact

Mathias Nittka, Ph.D.
Siemens Healthcare GmbH
DI MR DL ORTH
Erlangen
Germany
Phone: +49 9131 84 4460
mathias.nittka@siemens-healthineers.com